Physical origin of residual thermal stresses in a multilayer ceramic capacitor

Hyunho Shin, Jong-Sung Park, Kug Sun Hong, Hyun Suk Jung, Jung-Kun Lee, and Kyong Yop Rhee

Articles you may be interested in

Nonlinear acoustic effects in multilayer ceramic capacitors
AIP Conf. Proc. **1511**, 1462 (2013); 10.1063/1.4789214

Influence of thickness and number of dielectric layers on residual stresses in micromultilayer ceramic capacitors
J. Appl. Phys. **101**, 104117 (2007); 10.1063/1.2735412

Thermally induced viscoelastic stresses in multilayer thin films
J. Appl. Phys. **97**, 103521 (2005); 10.1063/1.1905797

Residual stress evolution in multilayer ceramic capacitors corresponding to layer increase and its correlation to the dielectric constant
J. Appl. Phys. **97**, 094504 (2005); 10.1063/1.1894602

Mechanical and thermal stresses in multilayered materials
J. Appl. Phys. **95**, 1780 (2004); 10.1063/1.1642289

Physical origin of residual thermal stresses in a multilayer ceramic capacitor

Hyunho Shin
Department of Ceramic Engineering, Kangnung National University, Kangnung 210-702, Korea

Jong-Sung Park and Kug Sun Hong[a)]
School of Materials Science and Engineering, Seoul National University, Seoul 151-744, Korea

Hyun Suk Jung and Jung-Kun Lee
Materials Science and Technology Division, Los Alamos National Laboratory, Los Alamos, New Mexico 87545

Kyong Yop Rhee
School of Mechanical and Industrial Systems Engineering, Kyunghee University, Yongin 449-701, Korea

The physical origin of the residual stresses developed in the ceramic layer of the active region in a multilayer ceramic capacitor was numerically investigated. The compressive in-plane stress components σ_{11} and σ_{22} originate without regard to the presence of the margins but rather from the difference in in-plane thermal shrinkage between ceramic and metal electrode. The out-of-plane stress component σ_{33} physically originates mainly through the presence of the housing margin; the presence of the lateral margin is a minor source: the more ceramic-rich margins hinder the apparent vertical shrinkage of the active region to yield tensile σ_{33}. © *2007 American Institute of Physics.*
[DOI: 10.1063/1.2713364]

I. INTRODUCTION

Multilayer ceramic capacitor (MLCC) is an essential passive compartment in modern electronic circuitry.[1] In general, a complicated residual stress state develops during fabrication because of the dissimilar thermal contraction behaviors of the two dissimilar materials, the dielectric ceramic and the metal electrodes. The knowledge of residual stress is important not only from the viewpoint of mechanical stability of the structure such as fatigue and lifetime, but also from the viewpoint of the dependency of the dielectric constant and loss on the residual stress.[2,3]

Regarding the influence of the residual stress on the dielectric constant of a MLCC, it has been reported that out-of-plane stress (vertical σ_{33} component) in a ceramic layer increases the dielectric constant when it is tensile.[4] In the cases of the in-plane stresses σ_{11} and σ_{22}, they increase the dielectric constant when they are compressive. This knowledge successfully explained the increase in the dielectric constant with the increase in the number of layers in a MLCC.[5] Therefore, it is important to uncover the physical origin of residual stresses in a MLCC, as such knowledge is very informative in the design of a MLCC.

In general, as-sintered MLCC structure experiences a polling process, tumbling process, and finally soldering process to mount on the circuit board. As the most predominant source to yield the residual stress state in a MLCC is the stress induced due to the thermal expansion mismatch during cooling after sintering, the current work aims to estimate the residual thermal stress developed in an as-sintered (and cooled) MLCC structure.

As for the approaches to the investigation of the residual stress state, the experimental determination of residual stress based on surface characterization methods such as indentation require the sectioning of the bulk device, which alters the stress state of the formerly bulk region, and thus stress information of bulk region obtained by this approach does not receive high reliability.[6] Near-surface characterization of a conventional x-ray diffraction is an acceptable tool to measure average residual stress of a few layers in the gauge volume provided the depth of x-ray penetration is sufficient to avoid the residual stress state at surface. Neutron diffraction yields a penetration depth of up to a few centimeters while, in general, sample gauge dimension of up to several millimeters is required,[7] and thus an effort to reduce the sample gauge dimension is required to investigate the stress state of a few-microns thick dielectric layer in MLCCs. A reliable method would be a high energy x-ray diffraction with synchrotron radiation, which has been developed to penetrate depths comparable to neutron diffraction, while reducing the size of the gauge volume dimension down to some 10 μm,[7,8] which thus can yield an averaged stress state of the dielectric layer in the gauge volume. Considering the fact that the residual stress is the self-equaling stress in a body, more detailed local stress information is necessary to extract the physical origin of the residual thermal stress in a MLCC structure unambiguously. A notable simple approach to investigate the stress state in MLCC structures is the numerical analysis based on the finite element method (FEM), which provides much detailed local stress information as compared to the experiment, and thus can provide an insight

[a)]Author to whom correspondence should be addressed; electronic mail: kshongss@plaza.snu.ac.kr
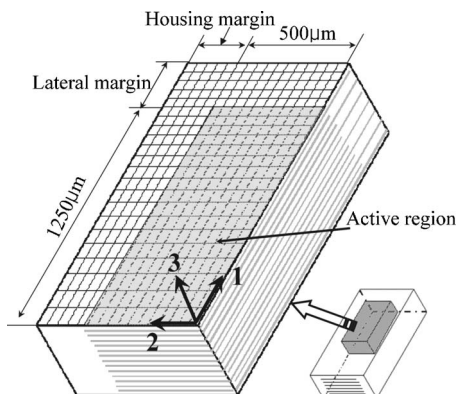
101, 063527-1

FIG. 1. Considered geometry of the MLCC and the 3D model used for calculation of residual stress.

which would be difficult to understand solely from the experiment. Further, the numerical approach overcomes the constraints of preparing specimens with unusual MLCC geometries like the ones considered in this work. Its reliability can be checked by comparing the experimental results for some limited regions of the bulk device such as the near surface region, information at which location can be suitably achieved by a conventional x-ray diffraction. Thus, FEM has been widely used to analyze the stress state in many nano-[9] and microstructures including MLCCs.[10–13] It has thus been adopted herein to elucidate the physical origin of the evolution of residual stresses in a MLCC and the numerical result has been compared with some experimental data in the literature.

II. NUMERICAL ANALYSIS

Figure 1 shows the considered geometry of a MLCC as well as a one-eighth space of the three-dimensional (3D) geometry that was modeled with appropriate boundary conditions to reduce computational load. The node points in 1–3 and 2–3 planes were fixed against movements along axes 2 and 1 directions, respectively. The thicknesses of the electrode and ceramic layers were 1 and 3 μm, respectively, and the 100 electrode and ceramic layers were modeled to simulate the structure with 200 electrode and ceramic layers. Both the housing margin (HM) and the lateral margin (LM) were modeled to have 0, 50, and 150 μm in width so that the influence of the respective margins on the residual stress evolution could be systematically monitored. Note that the dielectric performance of the MLCC structure is mostly realized in the active region where the ceramic and electrode layers are juxtaposed one by one. The number of electrodes (nickel) in the LM is only one half of that in the active region and the HM consists of a pure ceramic material (BaTiO$_3$).

The accurate prediction of magnitude of residual thermal stress in the as-sintered body requires the modeling of the core-shell structured of BaTiO$_3$ grains and the properties associated with textured grains together with the temperature-dependent material properties. However, as the purpose of the current work is to elucidate the physical origin of the thermal stress development, instead of accurate thermal stress level, influences of these minor sources were not taken
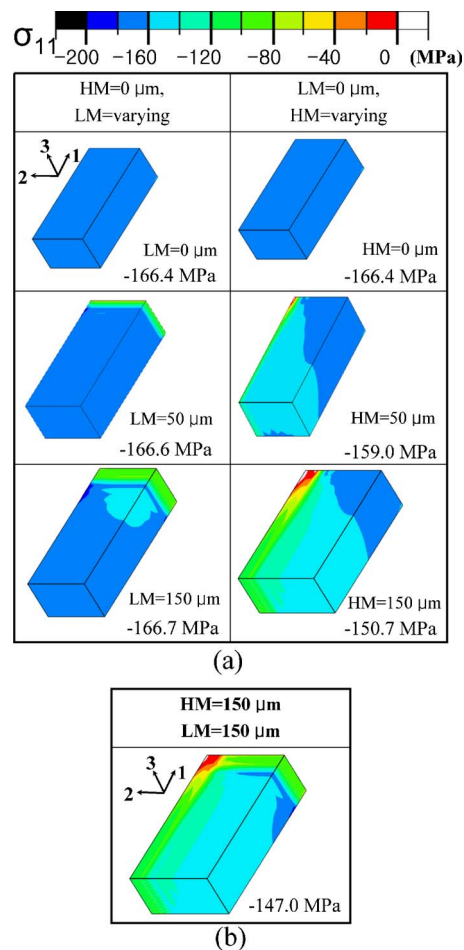

FIG. 2. (Color online) σ_{11} contour diagrams in the ceramic layers (a) for the cases when varying thickness of only the HM or the LM is present and (b) for the case when both 150 μm-thick HM and LM are present.

into account. Thus, the dielectric ceramic layer and the nickel electrode have been assumed to be polycrystalline and possess isotropic, homogeneous, and temperature-independent material properties. The elastic modulus, the coefficient of thermal expansion, and the Poisson ratio were 108 GPa, 11×10^{-6}/K, and 0.25, respectively, for the BaTiO$_3$ ceramic material, and were 207 GPa, 13.3 $\times 10^{-6}$/K, and 0.31, respectively, for the nickel electrode. The entire model experienced temperature change from the processing temperature (1250 °C) to the room temperature (20 °C). It means that the sintered materials (BaTiO$_3$ and Ni electrode) at 1250 °C were regarded as stress-free homogeneous media. The materials were allowed to shrink during cooling under the constraint of perfect bonding between the layers. The general purpose finite element package ABAQUS was used for the calculation with eight-node linear brick elements.

III. RESULTS AND DISCUSSION

A. In-plane residual thermal stress

The contour maps of the estimated residual thermal stress components in the ceramic layer are shown in Figs. 2–4. The magnitude of the stress in each frame indicates the average thermal stress in the active region of the dielectric
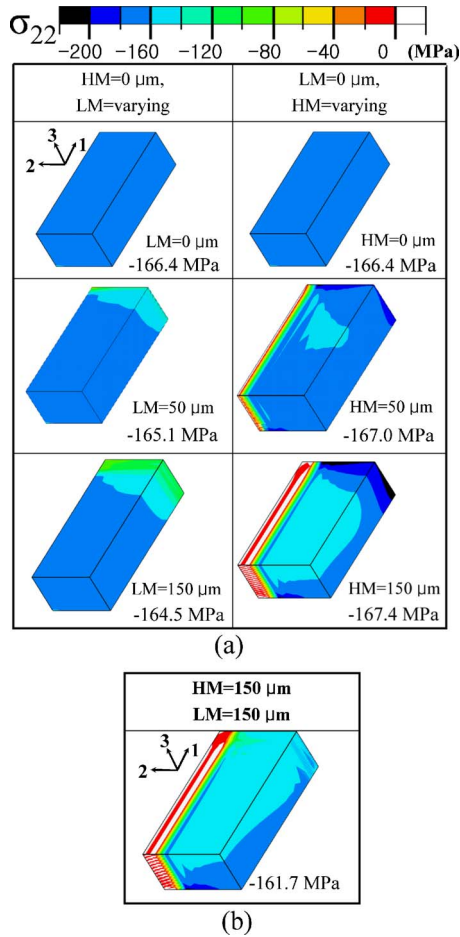
FIG. 3. (Color online) σ_{22} contour diagrams in the ceramic layers (a) for the cases when varying thickness of only the HM or the LM is present and (b) for the case when both 150 μm-thick HM and LM are present.
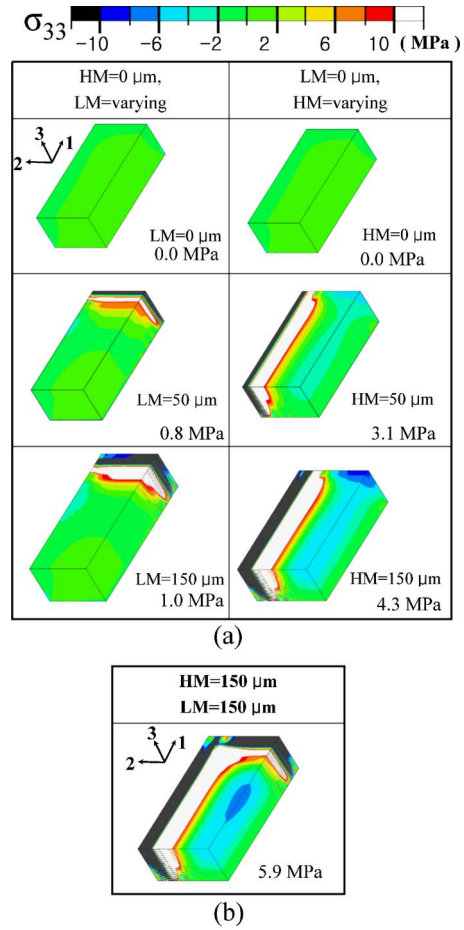

FIG. 4. (Color online) σ_{33} contour diagrams in the ceramic layers (a) for the cases when varying thickness of only the HM or the LM is present and (b) for the case when both 150 μm-thick HM and LM are present.

layer based on the assumptions employed in the modeling procedure. This magnitude is presented herein for the purpose of extracting physical origin of the residual thermal stress. As can be seen, the in-plane residual stress components σ_{11} and σ_{22} develop even when no margins exist. In Figs. 2 and 3, both are −166.4 MPa in the active region of the dielectric layer when no margins exist. This result means that they inherently arise without regard to the presence of either the HM or LM because the in-plane shrinkage of the nickel electrode itself in the active region is larger than the ceramic material during cooling.

The LM is a nickel/ceramic mixture and thus possesses effectively intermediate thermomechanical properties between the dielectric ceramic material and the nickel electrode. It tends to reduce the in-plane thermal contraction of the nickel electrode in the active region, although such tendency is smaller than the HM which is a pure ceramic material and takes larger volume than the LM. The reduced thermal contraction of the nickel electrode in the active region means a diminished compressive stress in the attached dielectric layer of the active region. Indeed the presence of the LM yields the zone with reduced magnitude of stress in the active region as seen in the left columns of Fig. 2(a) (σ_{11}) and Fig. 3(a) (σ_{22}). In the left column of Fig. 3(a), the magnitude of the average σ_{22} of the active region itself is thus

decreasing with increased thickness of the LM as well. In Fig. 2(a), however, the magnitude of the average σ_{11} increases although the amount of increase is very tiny. It is because there exists a locally stress-reinforced region at the upper left corner of the active region when LM=50 and 150 μm, although the volume of such reinforced region is very small. [In a separate analysis, when a thin HM (e.g., 50 μm-thick) additionally exists when LM=50 and 150 μm, which is indispensable in a practical MLCC, such local reinforcement disappears (not shown).] Thus, the presence of the LM itself decreases slightly (σ_{22}) or practically yields no apparent change (σ_{11}) in the magnitude of in-plane stresses in the active region.

The increase of the HM decreases the magnitude of the average in-plane stress components σ_{11} and σ_{22} more efficiently than the LM as seen in the right columns of Figs. 2(a) and 3(a) by the reason aforementioned. An interesting point is that the role of the HM in reducing the magnitude of average in-plane stress in the active region is more enhanced when the LM coexists although the role of the LM itself is not apparent. For instance, σ_{11} when HM=150 μm is −150.7 MPa [Fig. 2(a)] while σ_{11} when HM=150 μm and LM=150 μm is −147.0 MPa [Fig. 2(b)]. Also σ_{22} when HM=150 μm is −167.4 MPa [Fig. 3(a)] while σ_{22} when HM=150 μm and LM=150 μm is −161.7 MPa [Fig. 3(b)].

The reason for the synergistic effect is because the motion of the HM along axis 1 and 2, by the attached shrinking nickel electrode in the active region, is buttressed by the presence of the LM. This phenomenon resists the tendency of the nickel electrode in the active region to compress the dielectric layer in the same region along axis 1 (σ_{11}) and 2 (σ_{22}), respectively, thereby the synergistic effect results.

B. Out-of-plane residual thermal stress

For the investigation of the development of the out-of-plane stress component σ_{33}, the averaged value of σ_{33} in the ceramic layer of the active volume has been obtained. When no margins exist (Fig. 4), the magnitude of σ_{33} is negligible (the averaged value in the active region is 0.0 MPa), because there exists no apparent resistance to the vertical shrinkage of the MLCC structure. [Larger in-plane shrinkage of the electrode layers yields a driving force for slight vertical expansion of the ceramic layers due to the Poisson effect, and thus a very weak tensile stress state can develop (averaged σ_{33} in the active region is less than about 0.05 MPa).] This finding indicates that no physically meaningful σ_{33} develops without margins, unlike the cases of in-plane stress components, σ_{11} and σ_{22}.

When only the HM exists [the right column of Fig. 4(a)], the averaged value of σ_{33} in the active region increases notably from 0.0 to 4.3 MPa as the thickness of the HM increases, especially due to the highly tensile stress in the active region near the HM. Such phenomenon can be explained by the role of the HM. Vertical (along axis 3) shrinkage of dielectric ceramic layer in the active region is not influenced by the HM because the HM is the same ceramic material. However, the vertical shrinkage of the dielectric ceramic layer in the active region is hindered by the attached nickel electrode in the active region, because the vertical shrinkage of the nickel electrode is diminished by the HM. The hindered vertical shrinkage of the dielectric ceramic layer itself in the active region means a tensile stress in the ceramic layer. The development of tensile stress in the active region can also be understood by considering that the active region is a nickel/ceramic mixture and thus its effective thermal shrinkage in vertical direction is higher than the HM and thus its shrinkage is hindered by the HM, resulting in a tensile stress in the active region.

The presence of the LM [the left column of Fig. 4(a)] also increases the average σ_{33} in the active region from 0.0 to 1.0 MPa. This increase can also be explained by the fact that the LM is more ceramic-rich than the active volume because the number of electrodes in the LM is only one-half that of the active region. Thus the vertical shrinkage of the dielectric layer in the active volume is resisted by the LM as well by the same reason as the case of the HM, but the degree of hindrance (consequently the development of tensile σ_{33}) is less than in the case of the HM which is a pure ceramic material and takes more volume than the LM. Therefore, the major physical source for the development of tensile σ_{33} is the presence of the HM; a minor physical source for the development of tensile σ_{33} is the presence of the LM.

Like the case of in-plane residual thermal stress, the role of the HM in increasing the magnitude of average vertical stress in the active region is more enhanced when the LM coexists although the role of the LM itself is not significant, by the same reason as the case of in-plane stress. For instance, σ_{33} when HM=150 μm is 4.3 MPa [Fig. 4(a)] while σ_{33} when HM=150 μm and LM=150 μm is 5.9 MPa [Fig. 4(b)].

Although tensile stress develops in general in the active region and thus average σ_{33} value is positive, care has to be taken in experimental characterization of σ_{33} because a relatively weak compressive zone appears in the core of active region for the cases when only the HM exists [the right column of Fig. 4(a)] or the HM and LM coexist [Fig. 4(b)], which result from the complicated force equilibrium in the given MLCC structures.

C. Comparison with experiments

Now that the predicted residual thermal stresses have been presented, it is informative to compare the predicted values with existing experimental results elsewhere. As the dimension of the HM and LM are comparable to 150 μm in modern MLCC devices and the influence of the thickness on the residual stress is saturated after about 50 μm, the case when the LM and HM dimension is 150 μm in the current work has been compared with experiments. In Ref 6, when thicknesses of the nickel and dielectric layers were 2 and 4 μm, respectively, calculated σ_{11} was −152 MPa at the central dielectric layer in the active region, which is comparable to our result (−150.7 MPa) where the thicknesses were similar (1 and 3 μm, respectively). Indentation result in Ref. 6 was, however, only −24 MPa, resulting from the limitation of the surface characterization as the authors pointed out.

In Ref. 10, σ_{11} of a number of specimens were measured by x-ray and the values were in the range of −30 to −60 MPa depending on the type of specimens. Although the thicknesses of nickel electrode and dielectric layer were not specified explicitly, based on Ref. 11 by the same authors, the thickness of the dielectric layer is assumed to be about 25 μm, which is far thicker than the current work (3 μm). As the residual stress is a self equaling stress in a body, it is very sensitive to the thickness ratio of the nickel electrode and the dielectric layer. Therefore, the reason why the measured values (−30 to −60 MPa) in Ref. 10 was far lower than the predicted values in the current work may result from the fact that the thicker dielectric layer in Ref. 10 received less thermal contraction stress from nickel electrode during cooling. Although σ_{11} in the central zone of the active region is fairly insensitive to the number of layers in MLCC structure after about 50 layers in light of Ref. 5, the different number of layers in Ref. 10 (not specified explicitly) from the current work (200 layers) may contribute to the discrepancy as well.

In Ref. 14, σ_{11} and σ_{22} of as-sintered specimen were measured to be −164 and −177 MPa, respectively, by the x-ray method, which are similar to the current work (−150.7 and −161.7 MPa, respectively). However, direct comparison is limited as the thicknesses of the nickel electrode and the dielectric layer were not given in Ref. 14.

IV. CONCLUSION

The compressive in-plane stress components σ_{11} and σ_{22} originate without regard to the presence of margins, but rather from the difference in in-plane thermal shrinkage between the ceramic and the metal electrodes. The margins can only relieve the in-plane stress components. The out-of-plane stress component σ_{33} physically originates through the presence of margins. Ceramic-rich margins hinder the apparent vertical shrinkage of the active region to yield tensile σ_{33} in the ceramic layer of the active region, especially near the margins. The major physical source for the development of tensile σ_{33} is the presence of the HM; the LM provides a minor contribution.

ACKNOWLEDGMENT

[1] H. Kishi, Y. Mizuno, and H. Chazono, Jpn. J. Appl. Phys., Part 1 **42**, 1 (2003).

[2] Y. Nakano, T. Nomura, and T. Takenaka, Jpn. J. Appl. Phys., Part 1 **42**, 6041 (2003).

[3] K. Saito and H. Chazono, Jpn. J. Appl. Phys., Part 1 **42**, 6045 (2003).

[4] H. Shin, J.-S. Park, S.-J. Kim, H. S. Jung, and K. S. Hong, Microelectron. Eng. **77**, 270 (2005).

[5] J.-S. Park, S.-J. Kim, H. Shin, H. S. Jung, and K. S. Hong, J. Appl. Phys. **97**, 094504 (2005).

[6] J. M. J. den Toonder, C. W. Rademaker, and C.-L. Hu, J. Electron. Packag. **125**, 506 (2003).

[7] W. Reimers, M. Broda, G. Brusch, D. Dantz, K.-D. Liss, A. Pyzalla, T. Schmackers, and T. Tschentscher, J. Nondestruct. Eval. **17**, 129 (1998).

[8] A. Pyzalla, J. Nondestruct. Eval. **19**, 21 (2000).

[9] H. Shin, J.-B. Kim, Y.-H. Yoo, W. Lee, E. Yoon, and Y.-M. Yoo, J. Appl. Phys. **99**, 023521 (2006).

[10] K. Prume, K. Franken, U. Bottger, R. Waser, and H. R. Maier, J. Eur. Ceram. Soc. **22**, 1285 (2002).

[11] K. Prume, R. Waser, K. Franken, and H. R. Maier, J. Am. Ceram. Soc. **83**, 1153 (2000).

[12] K. Franken, H. R. Maier, K. Prume, and R. Waser, J. Am. Ceram. Soc. **83**, 1433 (2000).

[13] G. C. Scott and G. Astfalk, IEEE Trans. Compon., Hybrids, Manuf. Technol. **13**, 1135 (1990).

[14] G. de With and N. Sweegers, Wear **188**, 142 (1995).